Supporting Information

Flexible and Hollow Polypyrrole Foam with High Loadings of Metal-Organic Framework Nanowires for Wearable Supercapacitors

Ting Yue [a], Abdoulkader Ibro Douka [a], Kai Qi [a, b, c, *], Yubing Qiu [a, b, c], Xingpeng Guo [d], Bao Yu Xia [a, b, c]

[a] School of Chemistry and Chemical Engineering, Huazhong University of Science and Technology, Wuhan, 430074, P.R. China

[b] Key Laboratory of Material Chemistry for Energy Conversion and Storage (Ministry of Education), Huazhong University of Science and Technology, Wuhan, 430074, P.R. China

[c] Hubei Key Laboratory of Material Chemistry and Service Failure, Huazhong University of Science and Technology, Wuhan, 430074, P.R. China

[d] School of Chemistry and Chemical Engineering, Guangzhou University, Guangzhou, 510006, P.R. China

* Corresponding Authors: qikai@hust.edu.cn (K. Qi)

■ Experimental Section

Synthesis of polypyrrole hollow foam (PPy HF). Pyrrole was distilled and kept refrigerated in the dark before use. The purchased nickel foam was cut into a size of 12 cm × 10 cm and ultrasonized for 10 min in 1 M HCl, acetone, ethanol and ultra-pure water, respectively. The treated nickel foam was used as the working electrode, the platinum net was the counter electrode and the Ag/AgCl electrode was the reference electrode. Electrolyte solution configuration: 11 g of anhydrous sodium perchlorate was dissolved in 300 mL of aqueous solution and stirred until completely dissolved. Under the condition of sealing, N_2 was passed through to remove the oxygen in the above solution, and then 15 mL of pyrrole monomer was added. Under the above three-electrode condition, potentiostatic electrodeposition of 0.8 V vs. Ag/AgCl was conducted for 300 s. After electropolymerization, the nickel foam gradually turned black, and was rinsed with ultrapure water for 5 times. The resultant PPy coated nickel foam was fully etched in 1 M $FeCl_3$ for 5 h to remove the nickel skeletons and obtain the PPy hollow foam (PPy HF). Then, the PPy HF was taken out and rinsed with ultrapure water for 5 times. After that, 1.9 mg cm^{-2} of PPy HF with certain flexibility was obtained by blowing dry in N_2.

Synthesis of polypyrrole hollow foam/Ni-CAT nanowires (PPy HF/Ni-CAT-NWs). Ni-CAT-NWs is prepared by a modified method.[1, 2] 60 mg of nickel acetate was added into 20 mL of aqueous solution, and after it was completely dissolved, the PPy HF (2 cm × 2 cm) was soaked for 24 h. Then 20 mL of the prepared aqueous solution containing 42 mg of 2,3,6,7,10,11-hexahydroxytriphenylene (HHTP) was added and stirred slowly at 85 ^oC for 24 h. After the reaction, the product was taken out, and washed with deionized water and acetone for 5 times respectively to remove unreacted solvent and other impurities. The activated product was dried in a vacuum drying oven at 50 ^oC for 4 h to obtain the PPy HF/Ni-CAT-NWs composite, whose mass density was 3.7 mg cm^{-2}. It can be calculated that the mass loading of Ni-CAT-NWs was 1.8 mg cm^{-2}.

Synthesis of Ni-CAT powders. Similar to the preparation of the composite mentioned above, Ni-CAT

powders were synthesized without the addition of PPy HF. The obtained Ni-CAT powders were soaked in ultrapure water and acetone at 60 °C, and the water and acetone were changed every 5 h for 10 times. The activated Ni-CAT powders were dried in a vacuum drying oven at 60 °C for 12 h.

Preparation of Ni-CAT-NWs and Ni-CAT-powders electrodes. The Ni-CAT-NWs and Ni-CAT-powders electrodes were prepared by the traditional slurry coating method. The active materials were mixed with polyvinylidene fluoride and conductive carbon (80:10:10, w/w/w) in N-methyl-2-pyrrolidene solution by stirring into a sticky slurry. Then the slurry was coated onto the carbon cloth and dried at 50 °C overnight under vacuum. The mass loadings of Ni-CAT-NWs and Ni-CAT-powders were about 2 mg cm^{-2}, respectively.

Assembly of symmetric flexible all-solid-state supercapacitor. The gel electrolyte was prepared by mixing 2 g polyvinyl alcohol (PVA) and 4.25 g of LiCl in 20 mL DI water at 85 °C with stirring into a homogeneous, clear and sticky gel solution. LiCl can be well dissolved in PVA gel without crystallization during the gel drying process. The PVA-LiCl gel electrolyte could maintain excellent electrochemical and mechanical properties without the requirement to be wetted periodically. Two pieces of identical PPy HF/Ni-CAT-NWs electrodes were immersed into the above solution and then lifted up. Symmetrical two electrodes were allowed to assemble into a flexible supercapacitor device. The PVA/LiCl gel was acted as both the electrolyte and separator. Furthermore, to avoid moisture from the air, Paramembrane® was used to seal the supercapacitor device.

Characterizations. SEM and EDX were performed with a field-emission scanning electron microscope (FE-SEM, Nova NanoSEM 450) at an accelerating voltage of 10 kV. XRD patterns is conducted on a PANalytical B.V. x'pert3 powder X-ray diffractometer with Cu Kα radiation (λ = 1.5405 Å) at 30 kV and 20 mA from 10° to 35° with a scanning increment of 0.02°. TEM and high-resolution TEM images were obtained with a Tecnai G2 20 scope at an acceleration voltage of 200 kV. N_2 adsorptions experiments were measured on a Quantachrome Autosorb-1 automatic volumetric instrument. A liquid nitrogen bath (77 K) was used for

isotherm measurements. Ultra-high purity grade N_2 was used to the adsorption experiments. XPS spectra was collected by a monochromatic Al-Kα X-ray source (hv = 1486.6 eV, Kratos, AXIS-ULTRA DLD-600W). Thermogravimetric analysis (TGA) was performed on a Pyris 1 TGA (PerkinElmer Instruments) under air atmosphere at a heating rate of 5 °C min^{-1}. Infrared Spectroscopy (IR) was conducted on Equinox55 equipment.

Electrochemical measurements. The electrochemical performance of these electrodes were studied in a three-electrode cell in 3 M KCl aqueous electrolytes with Ag/AgCl and Pt plate as the reference electrode and counter electrode, respectively. All electrochemical measurements were performed on a CHI 660E electrochemical workstation. The areal capacitances were calculated using the following equations (1) to (2). Electrochemical performance of assembled flexible supercapacitor device were tested in a two-electrode configuration, where the areal energy (E) and power densities (P) were calculated using the following equations (3) to (4).

Areal capacitance (C_s)

$$C_s\left(\mathrm{F\ cm^{-2}}\right) = \int I_1 \mathrm{d}U / 2vSU \qquad (1)$$

$$C_s\left(\mathrm{F\ cm^{-2}}\right) = I_2 t / SU \qquad (2)$$

Energy density (E) and Power density (P)

$$E = \frac{CU^2}{(2 \times 3600)} \qquad (3)$$

$$P = E \times \frac{3600}{t} \qquad (4)$$

where I_1 (A) is the response current of CV, U (V) is the voltage window (voltage drop IR-drop has been considered for galvanostatic charging/discharging), v (V s^{-1}) is the scan rate, I_2 (A) is the discharging current, t (s) is the discharging time, S (cm^2) is the area of the electrode or supercapacitor device.

■ Supplementary Figures

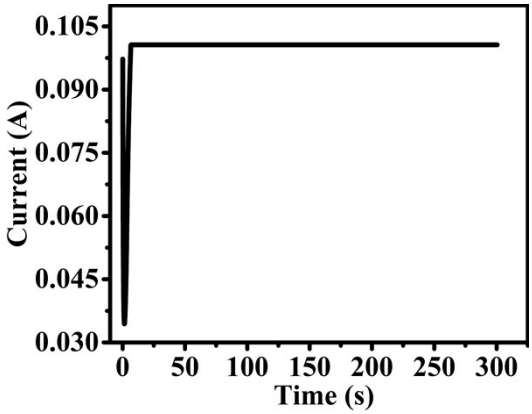

Figure S1. Current-time curve during the electrodeposition of PPy onto the nickel foam.

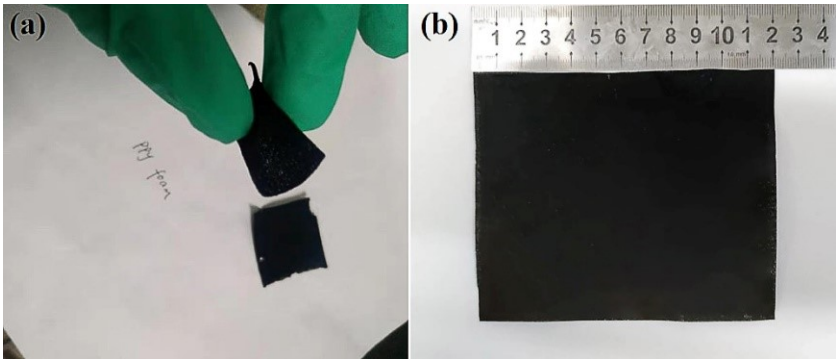

Figure S2. Digital photos of (a) PPy HF and (b) PPy HF/Ni-CAT-NWs.

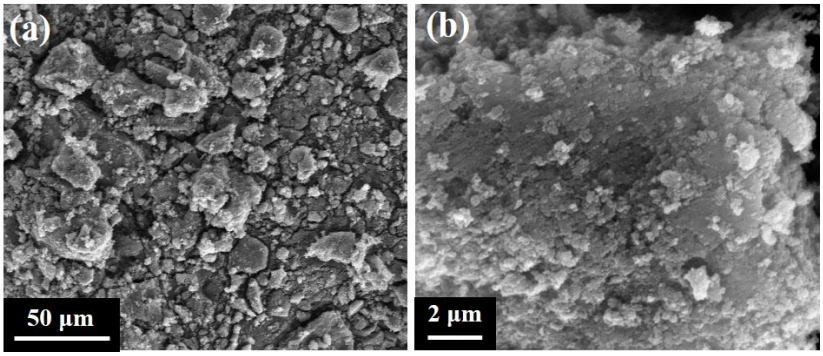

Figure S3. SEM images of different multiples for Ni-CAT powders.

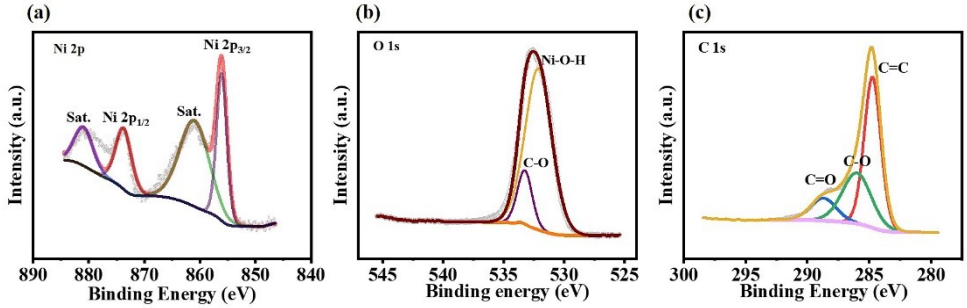

Figure S4. XPS spectra of (a) Ni 2p, (b) O 1s, and (c) C 1s in PPy HF/Ni-CAT-NWs.

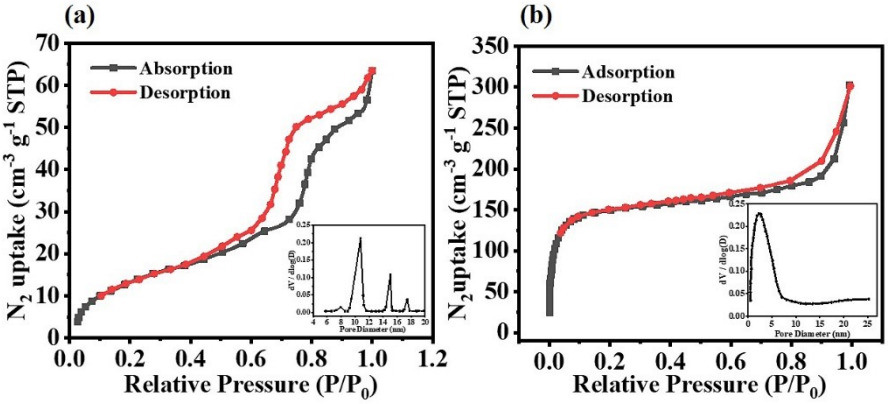

Figure S5. N_2 sorption isotherms of (a) PPy HF and (b) Ni-CAT-NWs.

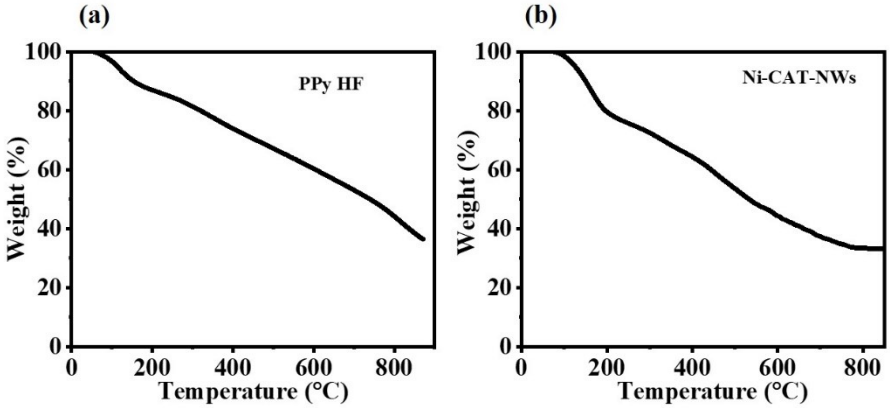

Figure S6. Thermal gravimetric analysis of (a) PPy HF and (b) Ni-CAT-NWs.

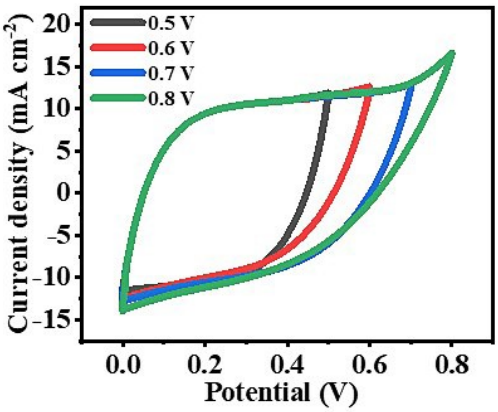

Figure S7. CV curves (at 5 mV s^{-1}) collected over various potentials for PPy HF/Ni-CAT-NWs.

As shown in Figure S7 for the CV curves (at 5 mV s^{-1}) of PPy HF/Ni-CAT-NWs, with the potential window increasing from 0-0.5 V to 0-0.8 V vs. Ag/AgCl, the polarization in the high potentials would obviously increase. Therefore, 0-0.5 V vs. Ag/AgCl is selected as the test potential window in the aqueous electrolyte.

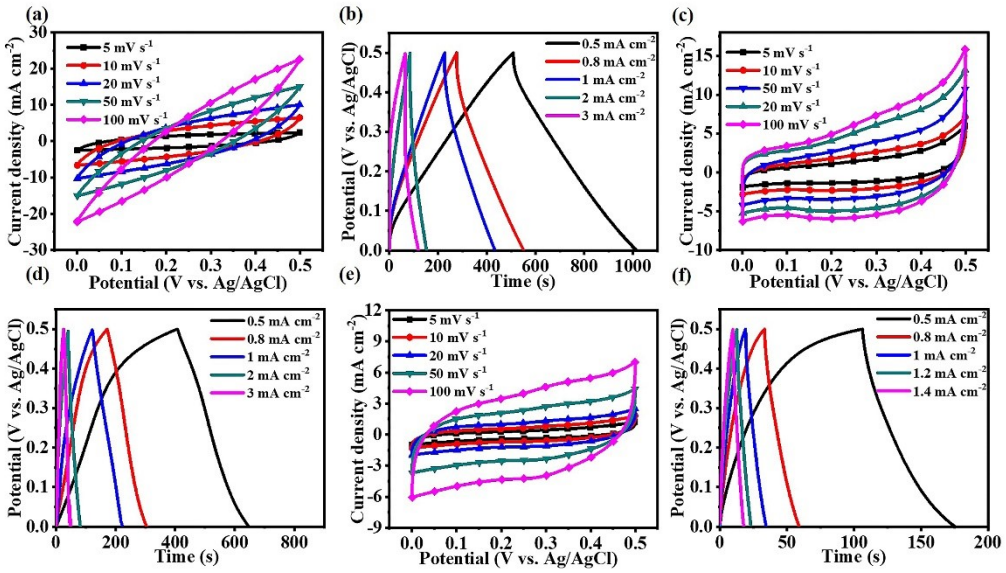

Figure S8. (a) CV and (b) GCD curves of PPy HF electrode. (c) CV and (d) GCD curves of Ni-CAT-NWs electrode. (e) CV and (f) GCD curves of Ni-CAT-powders electrode.

The mass specific capacitances of PPy HF/Ni-CAT-NWs, PPy HF, Ni-CAT-NWs, and Ni-CAT-powders electrodes are 283.9 F g^{-1}, 266.2 F g^{-1}, 133.3 F g^{-1} and 34.6 F g^{-1} respectively. The volume specific capacitances of PPy HF/Ni-CAT-NWs, PPy HF, Ni-CAT-NWs, and Ni-CAT-powders electrodes are 30.9 F cm^{-3}, 16.3 F cm^{-3}, 10.4 F cm^{-3} and 2.8 F cm^{-3} respectively.

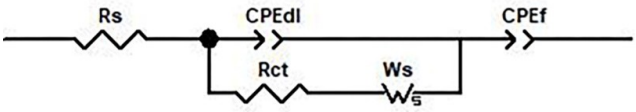

Figure S9. Equivalent circuit of the electrodes. R_s is electrolyte resistance; CPE_{dl} is electrical double-layer capacitance; R_{ct} is charge transfer resistance; W_s is Warburg diffusion process; CPE_f is pseudocapacitance.

The high-frequency part of EIS is a depressed tiny capacitive reactance arc composed of electric double layer capacitance CPE_{dl} and interface charge transfer resistance R_{ct}. As the frequency decreases, the electrochemical reaction gradually develops from the electrode interface to the inside. The middle-frequency part impedance is controlled by diffusion, which appears as a section of Warburg impedance in the equivalent circuit. When the frequency reduces to the low-frequency part, the electrochemical reaction extends to the entire electrode, the charge is saturated and remains unchanged with the potential changing. The impedance appears as a straight line approximately perpendicular to the real axis, which shows pure capacitive behavior.

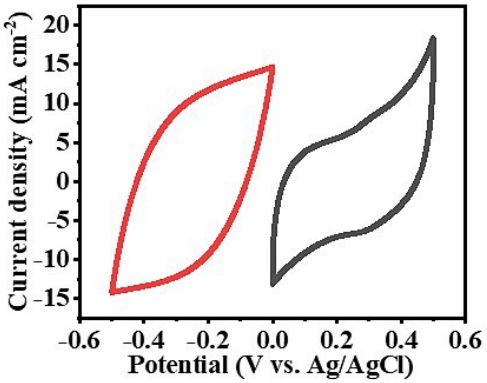

Figure S10. CV curves of PPy HF/Ni-CAT-NWs in a three-electrode system. The working potential window has been explored by cycling cathodically between 0 and -0.5 V and anodically between 0 and 0.5 V (vs Ag/AgCl).

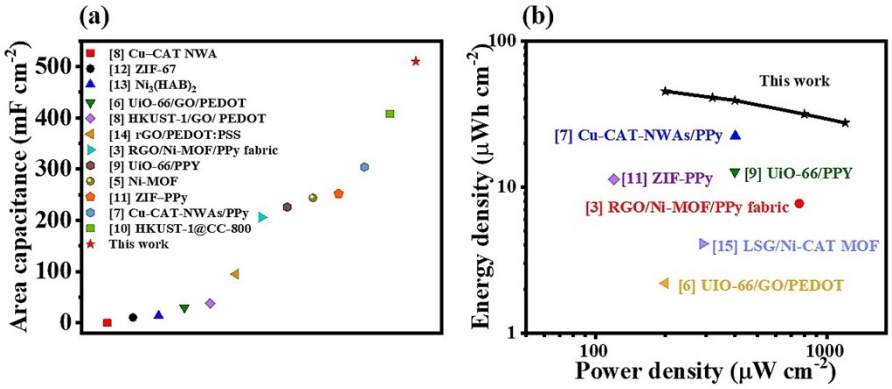

Figure S11. (a) Areal capacitance [3-14] and (b) Ragone plot with areal energy and power densities as well as comparison with some literature data.[3, 6, 7, 9, 11, 15]

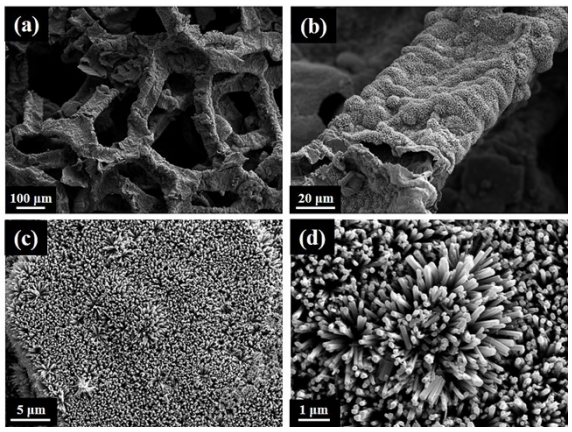

Figure S12. SEM images of PPy HF/Ni-CAT-NWs after cycled charging/discharging.

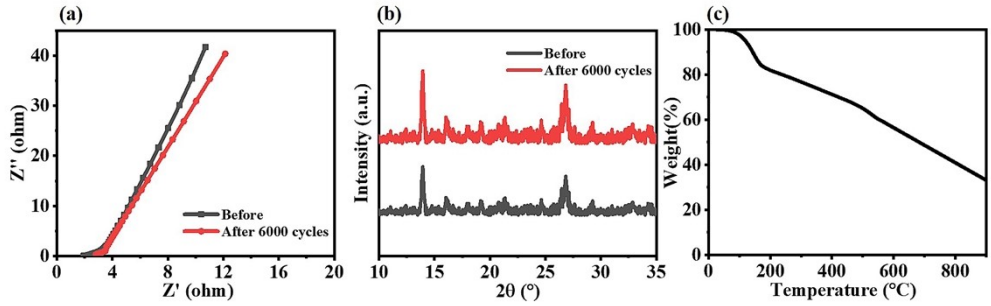

Figure S13. (a) EIS, (b) XRD and (c) thermal gravimetric analysis of PPy HF/Ni-CAT-NWs before and after 6000 cycles of charging/discharging.

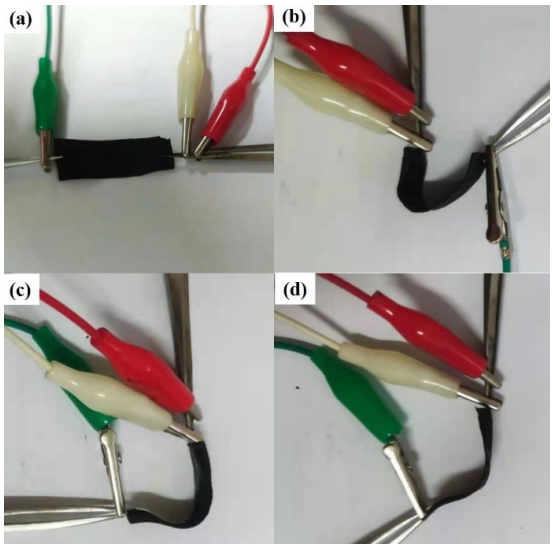

Figure S14. Different bending angles of the supercapacitor based on PPy HF/Ni-CAT-NWs.

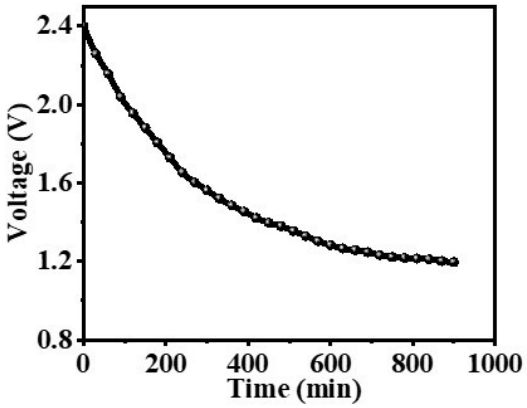

Figure S15. Self-discharging curve of three supercapacitors in series.

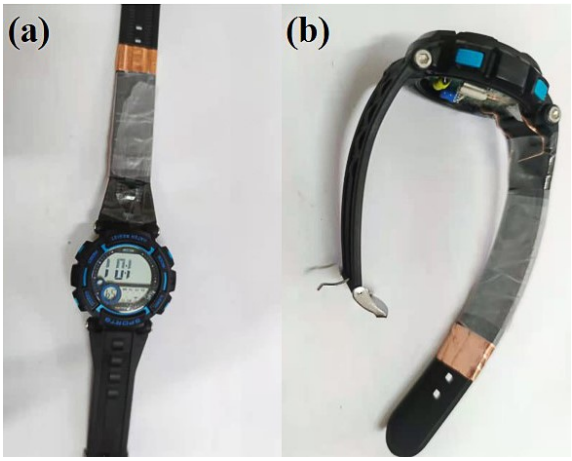

Figure S16. Digital photos of the supercapacitor with the area of 2 cm × 6 cm fabricated into a wearable wristband to drive an electronic watch.

■ References

[1] S. Zhou, X. Kong, B. Zheng, F. Huo, M. Stromme, C. Xu, *ACS nano*. **2019**, *13*, 9578-9586.

[2] M. Hmadeh, Z. Lu, Z. Liu, F. Gándara, H. Furukawa, S. Wan, V. Augustyn, R. Chang, L. Liao, F. Zhou, E. Perre, V. Ozolins, K. Suenaga, X. Duan, B. Dunn, Y. Yamamto, O. Terasaki, O. M. Yaghi, *Chemistry of Materials* **2012**, *24*, 3511-3513.

[3] C. Cheng, J. Xu, W. Gao, S. Jiang, R. Guo, *Electrochimica Acta*. **2019**, *318*, 23-31.

[4] D. Fu, H. Li, X.-M. Zhang, G. Han, H. Zhou, Y. Chang, *Materials Chemistry and Physics*. **2016**, *179*, 166-173.

[5] C. Yang, X. Li, L. Yu, X. Liu, J. Yang, M. Wei, *Chemical Communications*. **2020**, *56*, 1803-1806.

[6] D. Fu, H. Zhou, X.-M. Zhang, G. Han, Y. Chang, H. Li, *ChemistrySelect*. **2016**, *1*, 285-289.

[7] R. Hou, M. Miao, Q. Wang, T. Yue, H. Liu, H. S. Park, K. Qi, B. Y. Xia, *Advanced Energy Materials*. **2020**, *10*, 1901892.

[8] W.-H. Li, K. Ding, H.-R. Tian, M.-S. Yao, B. Nath, W.-H. Deng, Y. Wang, G. Xu, *Advanced Functional Materials*. **2017**, *27*, 1702067.

[9] K. Qi, R. Hou, S. Zaman, Y. Qiu, B. Y. Xia, H. Duan, *ACS Applied Materials & Interfaces*. **2018**, *10*, 18021-18028.

[10] D.-J. Li, S. Lei, Y.-Y. Wang, S. Chen, Y. Kang, Z.-G. Gu, J. Zhang, *Dalton Transactions*. **2018**, *47*, 5558-5563.

[11] X. Xu, J. Tang, H. Qian, S. Hou, Y. Bando, M. S. A. Hossain, L. Pan, Y. Yamauchi, *ACS applied materials & interfaces*. **2017**, *9*, 38737-38744.

[12] S. D. Worrall, H. Mann, A. Rogers, M. A. Bissett, M. P. Attfield, R. A. W. Dryfe, *Electrochimica Acta*. **2016**, *197*, 228-240.

[13] S. C. Wechsler, F. Z. Amir, *ChemSusChem*. **2020**, *13*, 1491-1495.

[14] C. Zhao, X. Jia, K. Shu, C. Yu, G. G. Wallace, C. Wang, *Journal of Materials Chemistry A*. **2020**, *8*, 4677-4699.

[15] H. Wu, W. Zhang, S. Kandambeth, O. Shekhah, M. Eddaoudi, H. N. Alshareef, *Advanced Energy Materials*. **2019**, *9*, 1900482.